ANN-Based Real-Time Optimal Voltage Control In Islanded AC Microgrids

1st Abd Alelah Derbas 2nd Chiara Bordin
Department of Computer Science
The Arctic University of Norway, UiT
Tromø, Norway
abd.a.derbas@uit.no chiara.bordin@uit.no

3rd Sambeet Mishra
Department of Electrical, IT and Cybernetics
University of South Eastern Norway (USN)
Porsgrunn, Norway
sambeet.mishra@usn.no

4th Frede Blaabjerg
Department of Energy
Aalborg University
Aalborg, Denmark
fbl@energy.aau.dk

***Abstract*—The purpose of this paper is to explore an innovative primary control strategy for a voltage source inverter (VSI). This strategy involves integrating an Artificial Neural Network (ANN) into the proportional resonant (PR) regulator within the inner loop of the primary control system. The primary objective is to regulate the output voltage and minimize deviations under various operating conditions, thereby enhancing the inverter's overall performance. The ANN, employed as a predictive analytic method, facilitates real-time tuning of the PR controller parameters. In addition, the outer level of primary control incorporates a droop control loop to distribute power among distributed generators (DG). This proposed approach reduces the converter control system's reliance on specific operating conditions and seamlessly accommodates varying loading conditions. To ensure adaptability and stability in various operating conditions, real-time simulations are implemented using OPAL-RT (OP4510), and the results demonstrate the efficacy of the proposed control strategy.**

***Index Terms*—Artificial Neural Network (ANN), Artificial intelligent control, Predictive analytic method.**

I. Introduction

In the ever-evolving landscape of microgrids, the integration of Distributed Energy Resources (DERs) is becoming increasingly prevalent, reshaping the dynamics of energy systems and emphasizing the critical importance of robust voltage control [13]. The surge in adoption of wind turbines, solar panels, and other DERs underscores the need for innovative control strategies to ensure stable and reliable microgrid operation [2]. In the midst of this significant shift towards DER-based energy systems, island microgrids face unique challenges in maintaining voltage stability, exacerbated by their highly dynamic load profiles, limited inertia, and the intermittent nature of renewable energy sources [3]. These challenges underscore the limitations of conventional Voltage Source Inverter (VSI) control methods, which often exhibit fixed or slow-adapting parameters, struggle with harmonic mitigation, and prove sensitive to unforeseen system uncertainties [4]. Recognizing these challenges, the integration of predictive analytics and Artificial Intelligence (AI) methods emerges as a promising avenue for enhancing VSI control in island microgrids [5]. Predictive analytics and AI not only provide a means of real-time learning and adaptation but also offer a pathway to overcome the limitations of conventional control methods. By combining the adaptability and learning capabilities of AI with the stability provided by conventional methods, intelligent controllers can be designed to address the unique intricacies of island microgrid operation [6], [7]. The advantages of employing AI methods in the context of VSI control for microgrids are multifaceted. Real-time learning and adaptation, facilitated by AI algorithms, enable continuous improvement, allowing the controller to anticipate and respond to dynamic load changes promptly [8]. This translates into enhanced voltage regulation, with reduced deviations and improved power quality by minimizing harmonic distortion, thereby ensuring better compatibility with connected loads [9]. The increased system stability achieved through AI-based control contributes to enhanced resilience against dynamic load disturbances, ultimately resulting in reduced operational costs through lower harmonic-related losses and improved overall efficiency [10]. Recent studies have explored the potential of AI in VSI control for microgrids, focusing on addressing stability, power quality, and control integration challenges. [4] and [11] both propose virtual impedance-based and adaptive droop control strategies, respectively, to enhance stability and improve power allocation accuracy. [12] discusses the potential of AI, particularly deep learning and deep reinforcement learning, in addressing the complex energy management issues in microgrids. [13] introduces an adaptive droop control and fuzzy PI control mechanisms for voltage and frequency control, aiming to reduce harmonic distortion and be independent of line parameters. These studies collectively highlight the potential of AI in addressing various challenges in VSI control for microgrids.

Current AI-based methods for VSI control in microgrids struggle with limited adaptability, complex algorithms, and often focus on single aspects like voltage regulation or harmonic mitigation. Our proposed solution integrates a ANN within a proportional resonant (PR) controller, addressing these limitations. By predicting system behavior and adaptively tuning the controller, our method simultaneously optimizes voltage regulation and harmonic mitigation, achieving less than 2% reduction in voltage deviations compared to conventional methods. The ANN's predictions further enhance prescriptive analytics for optimized control and resource allocation, sig-

This work is funded within the Aurora Center MASCOT

nificantly boosting microgrid efficiency and resilience. This methodology bridges predictive and prescriptive analytics [14], opening up promising avenues for further research and practical applications in diverse microgrid scenarios [15], [16].

II. AC Microgrid Modeling

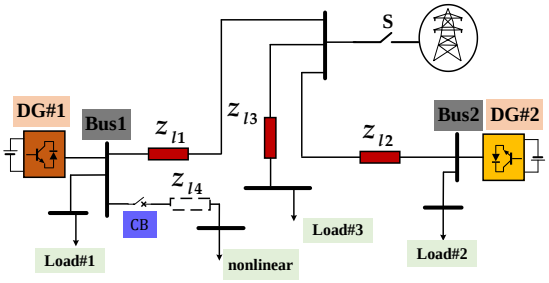

Fig. 1: The single-line diagram of the understudied ACMG

Figure 1 displays a schematic of the ACMG, featuring two DG units operating as voltage source converters (VSCs) supplying power to both local and remote loads. The ACMG operates in island mode, and each DG unit utilizes a decentralized control strategy for microgrid regulation, as depicted in Fig. 2.

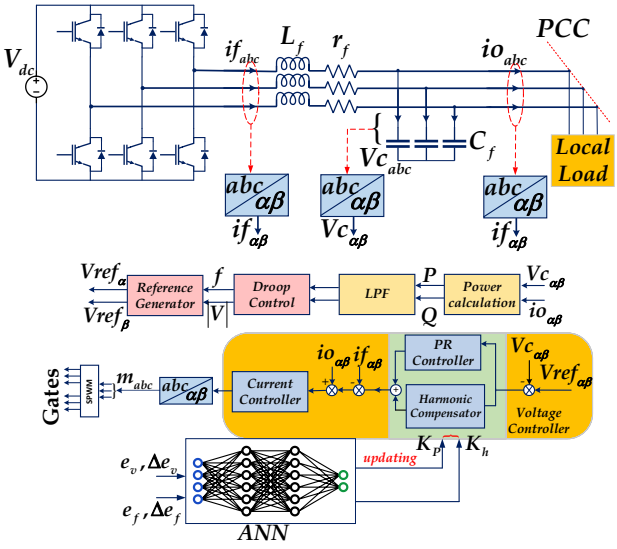

Fig. 2: Structure of the proposed control system.

A three-phase LC filter, connected to a load, aims to eliminate harmonics from the output voltage and current. The dynamic model of this filter, expressed in the $\alpha - \beta$ frame, is given by:

$$L_f \frac{dif}{dt} = vi - vc - i_f \cdot r_f$$
$$Cf \frac{dvc}{dt} = if - i_o \tag{1}$$

where L_f and C_f represent the inductor and capacitor of the filter, respectively. v_i and i_o denote the input voltage and output current of the filter, respectively. The input voltage v_i is connected to the dc-link voltage V_{dc} and the switching state vector.

To establish a feedback control system capable of adjusting load voltages amidst disturbances, the dynamic model is transformed into the stationary $\alpha - \beta$ frame using the Clarke transformation $\mathbf{T}$:

$$\dot{\mathbf{X}} = \mathbf{AX} + \mathbf{BU} + \mathbf{ED}, \qquad \mathbf{Y} = \mathbf{CX} \tag{2}$$

where $\mathbf{X}$, $\mathbf{U}$, $\mathbf{D}$, and $\mathbf{Y}$ are matrices representing state variables, inputs, disturbances, and outputs, respectively.

The output voltage in the $\alpha - \beta$ frame is expressed in the Laplace domain:

$$V_{c_{\alpha\beta}}(s) = M_{(2\times2)}(s)V_{i_{\alpha\beta}}(s) - N_{(2\times2)}(s)I_{o_{\alpha\beta}}(s) \tag{3}$$

with decoupled matrices $M_{(2\times2)}(s)$ and $N_{(2\times2)}(s)$.

The proposed control strategy focuses on the primary control, incorporating droop control as the outer loop and voltage control as the inner loop. The droop control loop generates reference signals for the voltage control, ensuring power-sharing for active and reactive power. The droop characteristics equation is given by:

$$f = f_0 - m(P_{av} - P_0) \qquad V = V_0 - n(Q_{av} - Q_0) \tag{4}$$

where f_0, V_0, m, and n are nominal frequency, voltage, and droop coefficients, respectively.

The voltage control loop, designed with double loops, sustains the bus voltage of the DG unit within acceptable limits. A feed-forward control loop mitigates the influence of load dynamics.

The current control employs a PI controller with parameters K_p and K_i adjusted for internal stability and VSC protection. The PR controller regulates voltage, providing steady-state tracking for the sinusoidal reference signal.

The PR controller's transfer function is expressed as:

$$G_{PR}(s) = K_P + \Sigma_{h=2n+1}^{\infty} \frac{K_h s}{s^2 + 2h\omega_c s + \omega_h^2}$$
$$n = 0, 1, 2, 3, ...\infty \tag{5}$$

where K_P and K_h represent the proportional and integral harmonic gains, respectively.

III. Methodology

An artificial neural network (ANN) is employed as a predictive analytic method to adjust these parameters based on operating conditions. The ANN is trained on a dataset of historical system data and is then used to predict the optimal parameters for the current operating conditions. This allows for improved system stability and performance. In our work, the ANN is designed with three layers: the input and output layers each have 2 nodes, and the hidden layer has 5 nodes.

A. Artificial neural network (ANN) modeling

PR control is employed in power electronic systems, to ensure that the converter output closely follows the sinusoidal reference waveform, and to reduce harmonics and minimizing distortion in the output voltage. However, in practice, tuning the parameters of a PR controller can be a challenging task. Achieving optimal performance requires careful adjustment of proportional and resonant gains, and this tuning process

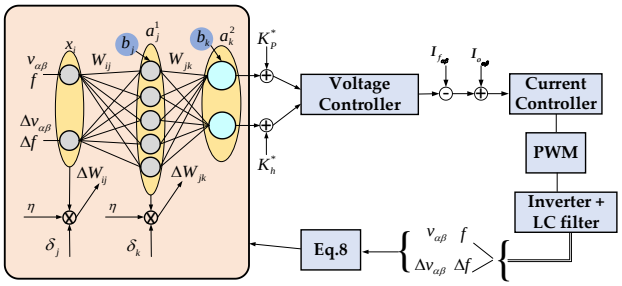

Fig. 3: The architecture of the ANN based voltage control of the VSC

may be complex and time-consuming, particularly for complex systems.

The ANN adjustor is used to adjust the parameters of proportional gain K_P and integral harmonic gain K_h based on the errors e_v and e_f and the change of error Δe_v and Δe_f, as shown in Fig. 2.

$$K_P = K_P^* + \Delta K_P \qquad K_h = K_h^* + \Delta K_h \tag{6}$$

where K_P^* and K_h^* are the reference values of ANN-PR-based controllers. K_P^* and K_h^* are calculated offline based on the Ziegler–Nichols method. In the proposed algorithm, a three-layer artificial neural network (ANN) is employed to update the controller coefficients K_P and K_h. The variables f and v_c are measured by sensors. As illustrated in Fig. 2, the inputs to the ANN, denoted as $e_{v,f}$ and $\Delta e_{v,f}$.

The architecture of the ANN based voltage control of the VSC is shown in Fig. 3 and described in Algorithm 1. As shown in Fig. 3, the inputs consist of the tracking error $e_v(t) = V_{ref_{\alpha\beta}} - v_{\alpha\beta}(t)$ and its rate of change $\Delta e_v = e_v(t) - e_v(t-1)$. Additionally, the error $e_f(t) = f_{ref} - f$ and its rate of change $\Delta e_f(t) = e_f(t) - e_f(t-1)$ are considered. The outputs ANN unit are denoted as ΔK_p and ΔK_h. The output of the j-th node in the hidden layer can be defined as:

$$a_j^{(1)} = \phi\left(Z_j^{(1)}\right) = \phi\left(\sum_{i=1}^{p} w_{ij} x_i + b_j\right) \tag{7}$$

x_i represents the input to the i-th node in the input layer. w_{ij} is the weight from the i-th input node to the j-th node in the hidden layer. $a_j^{(1)}$ and $Z_j^{(1)}$ represent the output and the weighted sum at the j-th node in the hidden layer, respectively. ϕ is the activation function. p the nodes number in the hidden layer.

The sigmoid function is chosen to represent the activation function

$$a_n^{(l)} = \phi\left(Z_n^{(l)}\right) = \frac{1}{1 + e^{-Z_n^{(l)}}}$$

where l represents the layer. $l = \{0, 2, 3\}$ for input, hidden and output layers, respectively. The objective during training process is to minimize the cost function E, as expressed:

$$E = \frac{1}{2} \sum_{i=1}^{p} e_i^2 \tag{8}$$

where p is the number of the nodes in the input layer. $e_i = x_{ref} - x_i$; where x_i, x_{ref} are the mearsured and the desired value at the i-th neuron in the input layer. The output of each layer can be calculated as:

$$\begin{aligned}
a_i^{(0)}(t) &= \phi\left(Z_i^{(0)}(t)\right) = x_i(t), i = 1, 2 \\
a_j^{(1)}(t) &= \phi\left(Z_j^{(1)}(t)\right) = \phi\left(\sum_{i=1}^{p} w_{ij} x_i(t) + b_j\right), j = 1, 2...5 \\
a_k^{(2)}(t) &= \phi\left(Z_k^{(2)}(t)\right) = \phi\left(\sum_{j=1}^{m} w_{jk} x_j^{(1)}(t) + b_k\right), k = 1, 2
\end{aligned} \tag{9}$$

where t is the t-th iteration, $a_j^{(1)}(t)$ and $a_k^{(2)}(t)$ are the output of the j-th and k-th node in the hidden and output layers, respectively. m is the nodes number in the hidden layer. The back-propagation algorithm is used to update the weights of the ANN accorading to the following [6]:

If y_k is the target output for the k-th node in the output layer. δ_k and δ_j are errors of the output and hidden layers.

$$\begin{aligned}
\delta_k &= (y_k - a_k^{(2)}) \cdot (a_k^{(2)} \cdot (1 - a_k^{(2)})) \\
\delta_j &= \delta_k \cdot w_{jk} \cdot (a_j^{(1)} \cdot (1 - a_j^{(1)})) \\
\Delta w_{jk} &= \eta \cdot \delta_k \cdot a_j^{(1)} \qquad \Delta w_{ij} = \eta \cdot \delta_j \cdot x_i
\end{aligned} \tag{10}$$

$$\begin{aligned}
w_{jk}(t+1) &\leftarrow w_{jk}(t) + \Delta w_{jk} \\
w_{ij}(t+1) &\leftarrow w_{ij}(t) + \Delta w_{ij}
\end{aligned} \tag{11}$$

Algorithm 1

1: **Given:** $w_{ij}(0)$, $w_{jk}(0)$, b_j, b_k, η
2: **for** each sampling x_i **do**
3: **Solve (9)** $\Rightarrow$ $a_j^{(1)}$, $a_k^{(2)}$
4: **end for**
5: **Ckeck:** $\Rightarrow$ Δ**e==0**
6: **for** each sampling input j **do**
7: **Solve (10)** $\Rightarrow$ δ_k, δ_j
8: **end for**
9: **Apply** Δw_{ij}, Δw_{jk} to update the weights (11)
10: $t \longrightarrow t+1$
11: **Repeat:** $2 \longrightarrow 9$

IV. Simulation and Results

TABLE I: Parameters of ACMG

Parameter	Value	Parameter	Value
r_f , L_f, C_f	0.1 Ω, 4.3 mH, 15 μF	T_S^*	20 μSec
S_{L1}, S_{L2}, S_{L3}	0.8, 1.5, 1.28 kVA	V_{ref}	400 V
r_{l1}, r_{l2}, r_{l3}	2.8, 2, 1.1 mΩ	f_{ref}	50 Hz
L_{l1}, L_{l2}, L_{l3}	0.44, 0.32, 0.17 mH	f_s	25 kHz

T_S^* is the sampling time

A comprehensive assessment of the proposed intelligent primary control approach was conducted using established simulation tools, including MATLAB SimPowerSystems and OPAL-RT with RT-LAB configuration. The simulations incorporated realistic scenarios and were applied to an microgrid (ACMG) with two VSC-based distributed generators (DGs), as depicted in Fig. 1. The desired voltage and frequency settings

were 400V and 50 Hz, respectively, with detailed ACMG parameters outlined in Table I. Two scenarios of dynamic load

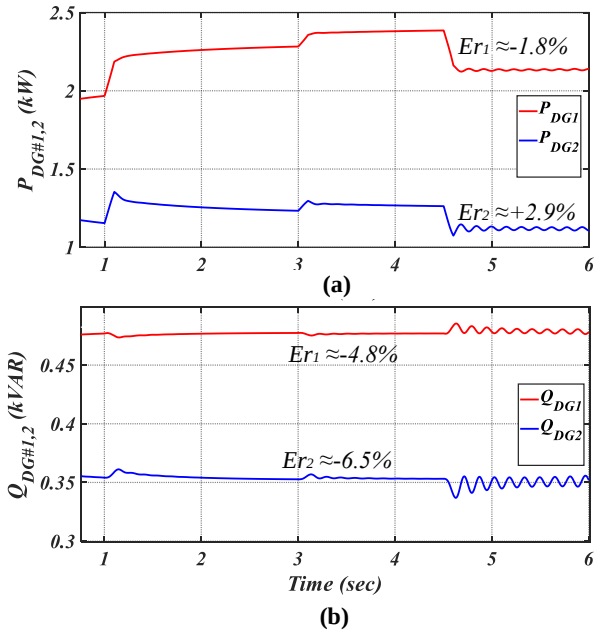

Fig. 4: Power-sharing among DGS during load changes in sequential steps using ANN-based PR controller: (a) Variations in Active Power, (b) Variations in Reactive Power.

changes were tested as follows:

A. Case I: Load changes in sequence steps

In this scenario, we assume the DGs operate under nominal loads and encounter *programmed, step-wise load changes*, including both increases and decreases. Specifically, Load #2 increases by 35% and 12% at times 1 and 3 seconds, respectively. Subsequently, it undergoes a 35% decrease at time 4.5 seconds. Fig. 4 illustrates the active and reactive power sharing between DG #1 and #2 during these sequential changes. The active power sharing errors are -1.8% and $+2.9\%$ for DG #1 and #2, respectively. The reactive power sharing errors are -4.8% and -7.2% for DG #1 and #2, respectively. Continuing Case I, the proposed controller demonstrates its effectiveness in reducing voltage and frequency errors, as well as harmonics, leading to superior performance, particularly under large dynamic load changes. Fig. 5 illustrates the output voltage variations of DG #1. As shown, the voltage error and total harmonic distortion (THD) voltage remain below 2% and 1%, respectively. Furthermore, despite the frequency variations, (Fig. 6 (a)) demonstrates that the frequency error is maintained below 0.007 Hz. (Fig. 6 (b)) shows the corresponding variations of the K_p and K_h coefficients in the controller.

B. Case II: Performance Comparison of Conventional and ANN-Based PR Controllers under Nonlinear Dynamic Load Conditions

To further validate the proposed control technique, we compared it with a PR controller under non linear loading conditions. In this scenario, we introduce a nonlinear load

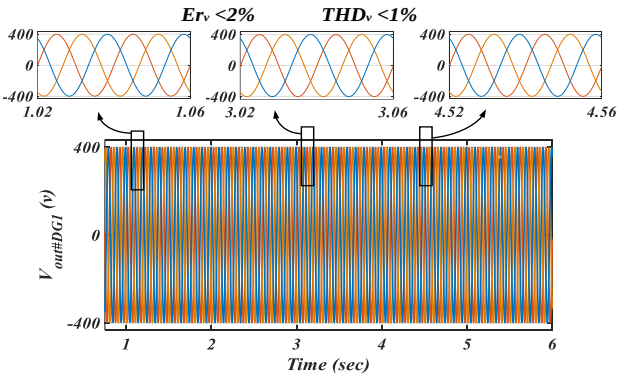

Fig. 5: Output voltage of DG#1 during load changes in sequential steps using ANN-based PR controller

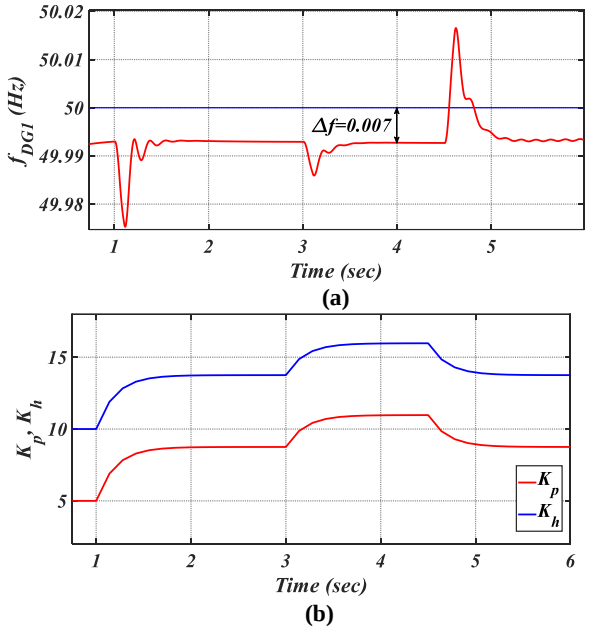

Fig. 6: (a) frequency variations, (b) K_p, K_h variations during load changes- using ANN-based PR controller

to further evaluate the proposed controller's robustness under dynamic load changes. A three-phase full-bridge rectifier with six pulses, modeled as a nonlinear load with 1.2 kVA power and 0.8 power factor, is connected to bus #1 at time 1 second in parallel with load #1. Figs. 7 depicts the output current variations for DG #1 and #2, respectively. The results, illustrated in Fig. 8 and Fig. 9 depict the output voltage variations in the presence of nonlinear dynamic changes in two cases using a conventional PI controller and using ANN-based PR controller. These figures clearly demonstrate the proposed controller's superior performance in handling the introduced nonlinear dynamic changes. As shown From Fig. 8 and Fig. 9 The total harmonic distortion (THD) for voltage is around 1% in case of using ANN-based PR controller, highlighting the controller's effectiveness in mitigating harmonic distortions caused by the nonlinear load. While THD value is 5.6% in case of using conventional PR controller. Furthermore, the error voltage is less than 2% by using ANN-based PR

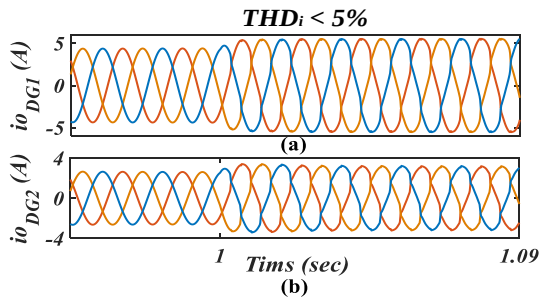

Fig. 7: Output current of DGs when connecting a nonlinear load- using ANN-based PR controller: (a) DG#1, (b) DG#2.

controller and approximately 5% by using a conventional PR controller. In the results, both controllers demonstrate

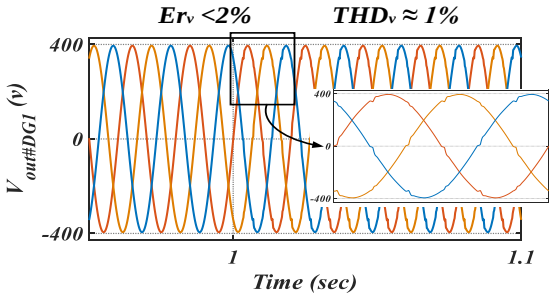

Fig. 8: Output voltage of DG#1 when connecting a nonlinear load- using ANN-based PR controller.

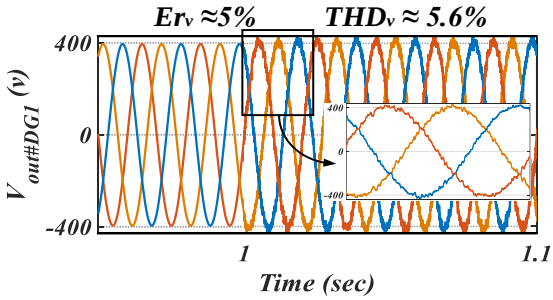

Fig. 9: Output voltage of DG#1 when connecting a nonlinear load- using a conventional PR controller.

compliance with the limitations outlined in the IEC 62040-3 standard and the IEEE 519 standard. However, the Adaptive Artificial Neural Network (AAN)-based PR controller stands out with a remarkable advantage. It consistently outperforms the conventional PR controller in terms of both voltage error and THD. This performance superiority proves its capability in regulating voltage and minimizing distortions, even in the presence of significant nonlinear load dynamics.

V. Conclusion

In this study, we applied real-time optimal voltage control using an ANN in the inner loop of the primary control level to adjust Proportional-Resonant (PR) controller parameters. The results highlight the remarkable effectiveness of the ANN-based PR controller, especially in regulating voltage and minimizing distortions under challenging load dynamics, including online learning with minimal computational complexity. The superior performance aligns with the IEC 62040-3 standard and the IEEE 519 standard, ensuring compliance and delivering greater stability and high-quality power. The reductions of 2% in voltage error and 1% in Total Harmonic Distortion (THD) offer several benefits in microgrid operation, including improved power quality for connected loads, reduced harmonic-related losses leading to increased energy efficiency and lower operational costs, and greater system stability and resilience under dynamic load conditions, ensuring smoother operations and enhanced reliability.

Acknowledgment

This research is supported by the UiT Aurora project MASCOT - Mathematical Structures in Computation.

References

[1] A. Muhtadi, et al., "Distributed Energy Resources Based Microgrid: Review of Architecture, Control, and Reliability", *IEEE Trans. Ind. Appl.*, vol. 57, no. 3, pp. 2223-2235, 2021, doi: 10.1109/TIA.2021.3065329.

[2] M. Ganjian-Aboukheili, et al., "Seamless Transition of Microgrids Operation From Grid-Connected to Islanded Mode", *IEEE Trans. Smart Grid*, vol. 11, no. 3, pp. 2106-2114, 2020, doi: 10.1109/TSG.2019.2947651.

[3] A. Hoke, et al., "Island Power Systems With High Levels of Inverter-Based Resources: Stability and Reliability Challenges", *IEEE Electr. Mag.*, vol. 9, no. 1, pp. 74-91, 2021, doi: 10.1109/MELE.2020.3047169.

[4] B. Keyvani-Boroujeni, et al., "Virtual Impedance-Based Droop Control Scheme to Avoid Power Quality and Stability Problems in VSI-Dominated Microgrids", *IEEE Access*, vol. 9, pp. 144999-145011, 2021, doi: 10.1109/ACCESS.2021.3122800.

[5] M. Alizadeh, et al., "Enhanced Distributed Event-Triggered Mechanism of Cyber-Switched Communications for Control of Islanded AC Microgrids", *IEEE Syst. J.*, vol. 17, no. 1, pp. 1501-1511, 2023, doi: 10.1109/JSYST.2022.3206026.

[6] A. A. Derbas, et al., "Adaptive Damping Control to Enhance Small-Signal Stability of DC Microgrids", *IEEE J. Emerg. Sel. Top. Power Electron.*, vol. 11, no. 3, pp. 2963-2978, 2023, doi: 10.1109/JESTPE.2023.3236809.

[7] A. A. Derbas, et al., "Intelligent Primary Control of Voltage Source Converters in AC Microgrids", *Proc. IECON 2022*, pp. 1-6, 2022, doi: 10.1109/IECON49645.2022.9969021.

[8] R. Dong, et al., "Output Control Method of Microgrid VSI Control Network Based on Dynamic Matrix Control Algorithm", *IEEE Access*, vol. 7, pp. 158459-158480, 2019, doi: 10.1109/ACCESS.2019.2949909.

[9] Y. Yu, et al., "Online Learning Based Voltage and Power Regulator for AC Microgrids", *IEEE Trans. Circuits Syst. II: Express Briefs*, vol. 68, no. 4, pp. 1318-1322, 2021, doi: 10.1109/TCSII.2020.3033891.

[10] E. Mohammadi, et al., "Review on Application of AI Techniques in Microgrids", *IEEE J. Emerg. Sel. Top. Ind. Electron.*, vol. 3, no. 4, pp. 878-890, 2022, doi: 10.1109/JESTIE.2022.3198504.

[11] L. Zhang, et al., "Adaptive Droop Control Strategy for Islanded Microgrid Based on Improved Particle Swarm Optimization", *IEEE Access*, vol. 8, pp. 3579-3593, 2020, doi: 10.1109/ACCESS.2019.2960871.

[12] T. Wu and J. Wang, "AI for Operation and Control: The Case of Microgrids", *The Electricity Journal*, vol. 34, no. 1, p. 106890, 2021, doi: 10.1016/j.tej.2020.106890.

[13] A. Muhtadi *et al.*, "Distributed Energy Resources Based Microgrid: Review of Architecture, Control, and Reliability", *IEEE Trans. Ind. Appl.*, vol. 57, no. 3, pp. 2223-2235, 2021, doi: 10.1109/TIA.2021.3065329.

[14] C. Bordin, "Mathematical optimization applied to thermal and electrical energy systems", Ph.D. thesis, alma, 2015.

[15] C. Bordin, et al., "Multihorizon approach for reliability-oriented network restructuring: Learning effects, construction time, and cables maintenance costs", *Renewable Energy*, vol. 168, pp. 878–895, 2021, Elsevier.

[16] A. A. Ibrahim, et al., "Pumped thermal electricity storage for active distribution network applications", *2017 IEEE Manchester PowerTech*, pp. 1–6, 2017, IEEE.